IEEE Access
Multidisciplinary | Rapid Review | Open Access Journal

Received January 12, 2021, accepted January 20, 2021, date of publication January 25, 2021, date of current version February 3, 2021.

Digital Object Identifier 10.1109/ACCESS.2021.3054519

Green Receivers for Massive MIMO Systems: A Joint Approach of Antenna Turn-Off and Multi-Level-Mixed-ADC Resolution Design

HOANG-YANG LU, WEI-LIN JIANG, AND CHENG ZHANG
National Taiwan Ocean University, Keelung 202301, Taiwan
Corresponding author: Hoang-Yang Lu (hylu@mail.ntou.edu.tw)

ABSTRACT In this paper, two green receivers with antenna turn-off and multi-level-mixed-ADC resolution design are proposed for massive MIMO systems, such as 5G networks and Internet of Things (IOT). For practicality, a generic power consumption model for massive MIMO receivers, including ADC resolution, symbol detection, and receiver circuits, is considered. The two proposed green receivers are formulated to minimize power consumption with respect to their individual spectral efficiency (SE) constraints, which are aimed at obtaining the optimal solution of the number of active receive antennas and corresponding multi-level-mixed-ADC resolutions. First, the proposed schemes enable the number of active receive antennas to be equal to the number of receive antennas. Second, a variant of the decremental searching and dynamic programming (DSDP) method is conducted to obtain the correspondingly optimal candidate of the multi-level-mixed-ADC resolution. Third, decrease the number of active receive antennas by 1 and then conduct the variant of DSDP again to search the correspondingly optimal resolution candidate of multi-level mixed ADCs. Fourth, repeat these mechanisms to obtain all optimal multi-level-mixed-ADC resolution candidates for different numbers of active receive antennas. Last, the number of active receive antennas and the corresponding multi-level-mixed-ADC resolution candidate, which achieve the minimum power consumption, are chosen as the optimal solution. In addition, a novel mechanism for accelerating the work of searching the number of turn-off antennas has been designed in the proposed receivers. The simulation results show that compared to DSDP, the two proposed green receivers can provide the advantage of the adjustable flexibility of power consumption with different SE requirements.

INDEX TERMS Analog-to-digital, maximum ratio combining, massive MIMO.

I. INTRODUCTION

Recently the demand of high Quality of Service (QoS) for modern communications has rapidly increased. Numerous researchers have been inspired to develop new technologies that are aimed at providing high reliability and throughput [1]–[6]. Massive multiple-input multiple-output (MIMO), in which the base station (BS) with hundreds of antennas serves tens of single-antenna users [7], is a potential technology. Due to the merits of providing high spatial multiplexing gain and spatial diversity without the extra bandwidth deployment, massive MIMO has been considered a promising approach for 5G and future wireless systems [8], [9]. In addition, from a mathematical viewpoint, massive MIMO also offers the following merits: 1) smoothing the channel effect of small-scale fading, 2) the column vectors of the channel matrix approaching mutually orthogonal as the number of BS's antennas increases, and 3) reduction of users' transmitted power consumption, contributed by the large number of receive antennas with the enhancement of receive antenna gains [10], [11]. Therefore, due to the demand of high QoS for current and future wireless communication systems, it is vital and interesting to investigate how to properly utilize massive MIMO technologies.

Massive MIMO has been proven to be capable of providing substantial spectral efficiency (SE) [12], [13]. However, the large number of antennas deployed in massive MIMO systems also cause a significant increase in power consumption, hardware cost, and system complexity [14], [15]. Especially for green communications, power consumption is

The associate editor coordinating the review of this manuscript and approving it for publication was Noor Zaman.

one of the most important concerns [15], [16]. Therefore, numerous studies have been motivated for power saving in massive MIMO systems [16]–[19]. The power consumed at the receivers of massive MIMOs mainly arises from the radio-frequency (RF) chains and baseband signal processing. The components of RF chains include amplifiers, analog-to-digital converters (ADCs), etc. [17]. The components of baseband signal processing include channel estimation and symbol detection, etc. [20]. In general, channel coefficients remain fixed with the assumption that the channel fading is block stationary. As a result, channel estimation is only conducted at the beginning of each block and is turned off at the residual part. Note that the meanings of a block can comprise several symbols or several packets. However, the mechanism of symbol detection is generally carried out once every symbol duration. Compared to channel estimation, symbol detection usually consumes more power [20]. To facilitate massive MIMO technologies for green communications, concurrently considering the power consumption of RF chains and symbol detection is a novel and important issue.

Furthermore, in the past two decades, many researchers have become devoted to the study of reducing the power consumption and hardware cost for MIMO systems and their variants [18], [21]–[25]. Some study approaches, including antenna selection and the deployment of low-resolution ADCs, have shown their potential. Using antenna selection in MIMOs, the transmitters/receivers only employ a feasible subset of the transmit/receive antennas for communications with slight performance degradation. Since only a subset of antennas is selected, only the corresponding subset of RF chains is active, and hence, receives the benefit of power saving [17], [25]. However, for practical implementation, antenna selection for massive MIMO systems suffers from the problems of computational complexity and hardware cost, which are mainly attributed to the deployment of the large number of antennas. For the deployment of low-resolution ADCs, antennas have also attracted considerable research attention due to their favorable properties, such as low hardware cost, feasibility of implementation, and low power consumption [18]–[24]. Especially due to the power consumption of each ADC that exponentially increases with the number of resolution bits, deploying low-resolution ADCs instead of high-resolution ADCs can save power. Currently, the kinds of low-resolution ADC deployments for massive MIMO systems include uniform low-resolution ADCs [18], two-level mixed ADC [19], and multi-level mixed ADCs [1]. For uniform low-resolution ADCs (*i.e.* one-level, low-resolution ADCs), the number of quantization bits of all ADCs is the same and low. For example, the number of quantization bits of all ADCs is 2. For two-level mixed ADCs, some receive antennas are equipped with the same low-resolution ADCs and other antennas are equipped with full-resolution ADCs. For multi-level mixed ADCs, different parts of ADCs with different level resolutions are concurrently available. In particular, [1] provides a dynamic programming scheme for designing the deployment of multi-level mixed ADCs to maximize the energy efficiency (EE) with respect to the SE constraints. However, this scheme is conducted with the assumption that all RF chains are active.

In this paper, two green receivers with antenna turn-off and multi-level-mixed-ADC resolution design are proposed for massive MIMO systems. In particular, the proposed two green receivers concurrently address the previously mentioned power consumption problems, which are one of the key issues of modern communication systems, such as 5G networks [4], Internet of Things (IOT) [2], and maritime communications [5]. The proposed green receiver is formulated to minimize the power consumption with the total SE (TSE) constraint or per-user SE (PUSE) constraint, which are aimed at obtaining the optimal solution of the multi-level-mixed-ADC resolutions and corresponding number of active receive antennas. Note that reducing the number of active receive antennas is equivalent to turning off receive antennas (i.e., RF chains), which introduces the benefit of power saving. Rich simulations and complexity analysis will be conducted to demonstrate that the proposed schemes can provide an advantage for the adjustable flexibility of power consumption with different SE requirements. The main contributions of the paper are summarized as follows:

- In most literature on massive MIMO systems, only power consumption for ADCs' resolutions is taken into consideration [1], [18], [19]. However, in addition to ADCs, some mechanisms such as symbol detection as well as circuits of receivers also require power in practice. Hence, to gain more insight into the issue, a new power consumption model with symbol detection, ADC resolutions and other circuit mechanisms are proposed.
- In fact, the formulations for the two proposed green receivers are NP-hard problems. To solve these problems, the proposed schemes first let the number of active receive antennas be equal to the number of all receive antennas. Then, a variant of the decremental searching and dynamic programming (DSDP) method [1] is conducted to find the corresponding optimal candidate of the multi-level-mixed-ADC resolution. Next, decrease the number of active receive antennas by 1 and then conduct the variant DSDP again to search the correspondingly optimal resolution candidate of ADCs. After that repeat the above mechanisms to find all optimal multi-level-mixed-ADC candidates for different numbers of active receive antennas. Finally, the above optimal candidates of ADCs' resolutions and the correspondingly active receive antennas, which achieves the lowest power consumption, will be chosen as the optimal solution.
- Furthermore, the proposed green receivers indeed require more computational complexity than DSDP [1], which is because they need to conduct the extra searching procedures to find the number of turn-offs antennas. Nevertheless, a novel mechanism for speeding up the works for searching the number of turn-off

TABLE 1. Comparisons among the proposed schemes and the priori methods [1], [18], and [19].

	power consumption model	ADC resoution type	goal
proposed	generic	multi-level	a joint optimization of antenna turn-off and ADC resolution vector
[18]	simplified	one-level	analysis of SE
[19]	simplified	two-level	analysis of SE
[1]	simplified	multi-level	optimization of ADC resolution vector

antennas has been designed in the proposed receivers. In addition, a proof has also been shown in Appendix to demonstrate the rationality of the speeding up mechanism.

- To assess the performance of the proposed schemes, rich simulations have been conducted. In particular, compared to DSDP [1] and the MRC receiver with two-level-ADC [19], the proposed green receivers can provide the advantage for the flexible adjustment of power consumption under different SE requirements, which means they are capable of consuming less power as the requirement of SE decreases.

Furthermore, for ease of reading, the comparisons of the proposed schemes with the priori methods in [1], [18], and [19] are shown in Table 1.

The remainder of the paper is organized as follows: Section II introduces the system model and some relevant preliminary knowledge. A detailed discussion of the two proposed green receivers is provided in Section III. Section IV demonstrates the simulation results and computational complexity. Conclusions are drawn in Section V.

Notation - Lower-case and upper-case bold letters denote vectors and matrices respectively. $|x|$ denotes the absolute value of x. $\mathbf{I}_N$ is the $N \times N$ identity matrix. $E\{\cdot\}$, $(\cdot)^T$, and $(\cdot)^H$ denote the expectation, the transpose, and the conjugate transpose operators respectively [26]. diag$\{\mathbf{A}\}$ is the diagonal matrix with only the diagonal terms of matrix $\mathbf{A}$. A complex Gaussian random variable distributed with mean μ and variance σ^2 is denoted as $\mathcal{CN}(\mu, \sigma^2)$.

Symbols and Definitions - For ease of reading, the symbols and their definitions used in the paper are listed in Table 2.

TABLE 2. List of the symbols and definitions.

Symbol	definition
M	amount of all receive antennas
$\tilde{M}$	amount of active receive antennas
K	number of single-antenna users
$\mathbf{H}$	wireless fading channel matrix
$\tilde{\mathbf{H}}$	sub-block of $\mathbf{H}$
$\mathbf{S}$	small-scale fading matrix
$\mathbf{L}$	large-scale fading matrix
β_i	large-scale fading coefficient for user i.
l_i	distance between user i and the BS.
γ	path loss exponent
$\mathbf{x}$	transmitted symbol vector
$\mathbf{y}$	received signal vector
$\mathbf{w}$	complex additive white Gaussian noise vector
σ_n^2	noise power of each entry of $\mathbf{w}$
$\mathbf{A}_a$	quantization matrix
$\mathbf{w}_a$	quantization noise vector
a_k	ADC's quantization coefficient for the kth active receive antenna
b	bits of ADC resolution
$\tilde{b}_m$	ADC resolution bits of the mth receive antenna
b_{max}	bits of ADC's highest resolution
$\mathbf{r}^{(\tilde{M})}$	multi-level-mixed-ADC resolution vector for $\tilde{M}$
$\mathbf{r}_{inner,opt}$	optimal $\mathbf{r}^{(\tilde{M})}$ of Inner Search Loop
$\mathbf{r}_{outer,opt}$	optimal $\mathbf{r}^{(\tilde{M})}$ of Outer Search Loop
$P_T^{(\tilde{M})}$	power consumption for $\tilde{M}$ and $\mathbf{r}^{(\tilde{M})}$
$P_{T,opt}^{(\tilde{M})}$	optimal $P_T^{(\tilde{M})}$
$P_{full}^{(M)}$	power consumption for M with full-resolution ADCs
μ_0	Flops for the computational complexity of symbol detection
P_d	power consumption for each Flop
P_b	a constant for the power consumption of ADCs' resolutions
P_c	circuit power of one RF chain
$R_k^{(\tilde{M})}$	average SE of user k for $\tilde{M}$ and $\mathbf{r}^{(\tilde{M})}$
$\Theta_T^{(\tilde{M})}$	total SE for the corresponding $P_T^{(\tilde{M})}$, and $\Theta_T^{(\tilde{M})} = \sum_{k=1}^{K} R_k^{(\tilde{M})}$
$\Theta_{full}^{(M)}$	total SE for the corresponding $P_{full}^{(M)}$
$\Theta_{T,opt}^{(\tilde{M})}$	optimal $\Theta_T^{(\tilde{M})}$
η	constant, $0 < \eta \leq 1$
η_k	constant for user k, $0 < \eta_k \leq 1$
$\eta_{average}$	average of $\eta_1 \cdots \eta_K$
Θ_{con}	total SE constraint and $\Theta_{con} = \eta \times \Theta_{full}^{(M)}$
$\Theta_{con,k}$	SE constraints for user k

II. PRELIMINARIES

A. SYSTEM MODEL

Consider a massive MIMO system where the BS uses M receive antennas to serve K single-antenna users. In general, each receive antenna is equipped with a RF chain, which may contains amplifiers, mixers, and an ADC. For brevity, we assume that the K users simultaneously send their individual symbols via a wireless channel over the M receive antennas of the BS. Further, let the $M \times K$ wireless channel matrix between the BS and the users be $\mathbf{H} = \mathbf{S}\mathbf{L}^{\frac{1}{2}}$, and its entry $h_{ij}, 1 \leq i \leq M, 1 \leq j \leq K$ denotes the channel coefficient between the ith receive antenna and the jth transmit antenna; $\mathbf{S}$ is the $M \times K$ small-scale fading matrix, whose elements are distributed with $\mathcal{CN}(0, 1)$ [20]; and $\mathbf{L} = \text{diag}\{\beta_1, \beta_2, \cdots, \beta_K\}$ is the $K \times K$ diagonal matrix, whose entries model the large-scale fading effect and ith diagonal entry $\beta_i = z_i l_i^{-\gamma}$, where z_i, l_i and γ are the log-normal random variable, the distance from the ith user to the BS, and the path loss exponent, respectively [19], [20]. For simplicity, it is assumed that the K transmitted symbols are mutually uncorrelated. In addition, it is also assumed that the BS has the perfect information of the channel matrix. The baseband received signal can be expressed as [1], [10],

$$\mathbf{y} = \mathbf{H}\mathbf{x} + \mathbf{w}, \tag{1}$$

where $\mathbf{x} = [x_1, x_2, \cdots, x_K]^T$ is the transmitted symbol vector and the element $x_k, k = 1 \cdots, K$, is the information symbol sent from user k; and $\mathbf{w}$ is the $M \times 1$ complex additive white Gaussian noise (AWGN) vector, whose elements are distributed with $\mathcal{CN}(0, \sigma_n^2)$ [20]. Due to the large number of antennas deployed at the receivers of massive MIMO systems, the physical footprint of the antenna arrays needs to be smaller to fit the compact demand. This requirement may cause severe mutual-coupling and correlation effects between adjacent antenna elements, which will lead to performance degradation [27]–[29]. Mutual-coupling is a vital issue in massive MIMO systems but beyond the scope of this paper.

TABLE 3. The quantization coefficient c_b for different ADC resolution bits b.

b	1	2	3	4	5
c_b	0.6366	0.8825	0.96546	0.990503	0.997501

B. RECEIVER WITH MULTI-LEVEL-MIXED-ADC

In massive MIMO systems, the large number of receive antennas leads to a large number of corresponding RF chains. As a result, the amount of power for launching the RF chains is unavoidably large. Because an ADC consumes the main power among the components of an RF chain, powerful schemes have been proposed recently to change high-resolution ADCs to low- or mixed-resolution ADCs for power saving [18], [19]. However, using low- or mixed-resolution ADCs will cause the received signal to experience quantization noise [20]. For tractability of analysis, we adopted the additive quantization noise model (AQNM) [1], [18], [19]. The quantized result of the received signal in (1) can be approximated as

$$\mathbf{y}_a = Q_a(\mathbf{y}) \approx \mathbf{A}_a\mathbf{y} = \mathbf{A}_a\mathbf{H}\mathbf{x} + \mathbf{A}_a\mathbf{w} + \mathbf{w}_a, \tag{2}$$

where $Q_a(\cdot)$ represents the quantization operation; $\mathbf{A}_a = \text{diag}\{a_1, a_2, \cdots a_M\}$, whose $a_k, k = 1 \cdots M$, is the quantization coefficient of the kth ADC and depends on the corresponding ADC resolution bits b, $1 \le b \le b_{max}$. For $1 \le b \le 5$, the values of the ADC quantization coefficients c_b are shown in Table 3 and approximated by $1 - \frac{\pi\sqrt{3}}{2}2^{-2b}$ for $b > 5$ [19]. For example, when $b = 2$ for the kth receive antenna, the corresponding a_k is c_2, *i.e.* $a_k = 0.8825$. $\mathbf{w}_a$ is the quantization noise vector, and with AQNM, is distributed with $\mathcal{CN}(0, \mathbf{R}_{\mathbf{w}_a})$, where $\mathbf{R}_{\mathbf{w}_a} = \mathbf{A}_a(\mathbf{I}_M - \mathbf{A}_a)\,\text{diag}(\mathbf{H}\mathbf{H}^H + \mathbf{I}_M)$ [1], [19]. The ith diagonal element of $\mathbf{R}_{\mathbf{w}_a}$ is the ADC quantization noise power for the ith receive antenna, $i = 1, \cdots M$.

C. POWER CONSUMPTION

For the receivers of the BSs in massive MIMO systems, the total power consumption is generally determined by three mechanisms: symbol detection, resolutions of ADCs, and other circuits of each receive antenna. For $\tilde{M}$ active receive antennas, the total power consumption can be expressed as [16]

$$P_T^{(\tilde{M})} = P_d \times \mu_0 + P_b \sum_{m=1}^{\tilde{M}} 2^{\tilde{b}_m} + P_c \times \tilde{M}, \tag{3}$$

where $\tilde{M} \le M$; P_d is the power consumption for each Flop. A Flop is the unit of a complex multiplication or an addition [26]; μ_0 represents the Flops for the computational complexity of symbol detection at the receiver; $\tilde{b}_m$ is the ADC resolution bits of the mth receive antenna; P_b is a constant for the power consumption of ADCs' resolutions, whose units are watts; and P_c represents other circuit power of one RF chain. Note that most existing works generally only consider the power consumption of ADCs [1], [19]. For practicality, the new generic model of power consumption in (3) is proposed in this paper.

D. SPECTRAL EFFICIENCY FOR MAXIMUM RATIO COMBING

Studies have shown that massive MIMOs can provide the merit of the favorable propagation condition, i.e., $\frac{1}{\tilde{M}}\tilde{\mathbf{H}}^H\tilde{\mathbf{H}} \approx \mathbf{D}_g$, if $\tilde{M} \gg K$, where $\tilde{\mathbf{H}}$ is the $\tilde{M} \times K$ sub-block matrix of $\mathbf{H}$ in (1) as $\tilde{M}$ receive antennas are active; and $\mathbf{D}_g$ is a diagonal matrix [10]. Due to the merit, massive MIMOs cause the signals that are sent from the users to be almost in parallel, and hence, less interference occurs at the receiver of the BS. Therefore, Maximum Ratio Combing (MRC) detection becomes popular for massive MIMO systems due to its low complexity. Using MRC (2) for symbol detection, the estimated result can be expressed as $\mathbf{z} = \tilde{\mathbf{H}}^H\tilde{\mathbf{y}}_a$, where $\tilde{\mathbf{y}}_a$ is the corresponding $\tilde{M} \times 1$ quantized result of the received signal. As a result, the computational complexity for MRC is $\tilde{M} \times K$ complex multiplications and $\tilde{M} \times (K-1)$ complex additions. Hence, the complexity is $\tilde{M} \times (2K - 1)$ Flops [26]. Because generally $\tilde{M} \gg K \ge 1$, the complexity is approximated to $2\tilde{M}K$ Flops. Furthermore, the kth element of $\mathbf{z}$ is expressed as $z_k = \tilde{\mathbf{h}}_k^H\mathbf{A}_a\tilde{\mathbf{h}}_k x_k + \tilde{I}_k$, where $\tilde{\mathbf{h}}_k$ is the kth column vector of $\tilde{\mathbf{H}}$ and $\tilde{I}_k = \sum_{i=1, i\neq k}^{K} \tilde{\mathbf{h}}_k^H\mathbf{A}_a\tilde{\mathbf{h}}_i x_i + \tilde{\mathbf{h}}_k^H\mathbf{A}_a\mathbf{w} + \tilde{\mathbf{h}}_k^H\mathbf{w}_a$ is the corresponding summation of interference and noise. For $\tilde{M}$ active receive antennas, the correspondingly average SE of user k can be written as $R_k^{(\tilde{M})} \approx E\{\log_2\big(1 + \frac{|\tilde{\mathbf{h}}_k^H\mathbf{A}_a\tilde{\mathbf{h}}_k|^2}{\sum_{i=1,i\neq k}^{K}|\tilde{\mathbf{h}}_k^H\mathbf{A}_a\tilde{\mathbf{h}}_i|^2 + \tilde{\mathbf{h}}_k^H\mathbf{A}_a^2\tilde{\mathbf{h}}_k + \tilde{\mathbf{h}}_k^H\mathbf{R}_{\mathbf{w}_a}\tilde{\mathbf{h}}_k}\big)\}$. Further, using the result in [1], this expression can be rewritten as

$$R_k^{(\tilde{M})} \approx \log_2\big(1 + \frac{\beta_k(\alpha_1^2 + \alpha_2)}{\gamma\alpha_1 - 2\beta_k\alpha_2}\big), \tag{4}$$

where $\alpha_1 = \sum_{m=1}^{\tilde{M}} a_m$; $\alpha_2 = \sum_{m=1}^{\tilde{M}} a_m^2$; and $\gamma = 1 + \beta_k + \sum_{j=1}^{K}\beta_j$. In addition, the TSE is $\Theta_T^{(\tilde{M})} = \sum_{k=1}^{K} R_k^{(\tilde{M})}$, whose corresponding number of active receive antennas is $\tilde{M}$ and ADC resolution coefficients are $a_m, m = 1 \cdots \tilde{M}$.

Furthermore, we can observe from (4) that the definitions of α_1 and α_2 are not determined by a specific receive antenna but the ADC quantization coefficients of active receive antennas. Therefore, (4) can be further re-expressed as

$$R_k^{(\tilde{M})} \approx \log_2\big(1 + \frac{\beta_k((\sum_{i=1}^{b_{max}} c_i r_i)^2 + \sum_{i=1}^{b_{max}} c_i^2 r_i)}{\gamma\sum_{i=1}^{b_{max}} c_i r_i - 2\beta_k\sum_{i=1}^{b_{max}} c_i^2 r_i}\big), \tag{5}$$

where r_i denotes the number of active receive antennas, whose ADC resolution bits are i and the corresponding resolution coefficient c_i is shown in Table 3. Furthermore, because the number of active receive antennas is $\tilde{M}$, the result $r_1 + r_2 \cdots + r_{b_{max}} = \tilde{M}$. Likewise, the power consumption in (3) can be further re-expressed as

$$P_T^{(\tilde{M})} = P_d \times 2\tilde{M}K + P_b\sum_{i=1}^{b_{max}} 2^i r_i + P_c \times \tilde{M}, \tag{6}$$

where $2\tilde{M}K$ in (6) is the computational complexity required for conducting MRC [16]. Similarly, we can also observe from (6) that $P_T^{(\tilde{M})}$ is determined by the number of active

receive antennas and their ADC resolution bits. Hence, $P_T^{(\tilde{M})}$ is also not affected by a specific receive antenna.

III. THE PROPOSED SCHEME

In this section, two new green receivers for massive MIMO systems are proposed to minimize power consumption with respect to different SE constraints, which is aimed at searching for the optimal solution of multi-level-mixed-ADC resolutions and the corresponding number of active receive antennas. Note that turning off active receive antennas (i.e., RF chains) is equivalent to reducing the number of active receive antennas, which will save power. The details of the two proposed schemes are provided as follows:

A. GREEN RECEIVER WITH TOTAL SPECTRAL EFFICIENCY (GR-TSE) CONSTRAINT

To provide more insight into power consumption, the new generic model in (6) is considered, which consists of the power consumption of MRC symbol detection, ADC resolutions, and other circuit power of each active receive antenna. In addition, denote $\mathbf{r}^{(\tilde{M})} = [r_1, r_2, \cdots, r_{b_{max}}]^T$ as the multi-level-mixed-ADC resolution vector, in which b_{max} is a full-resolution ADC and $r_i, i = 1, \cdots, b_{max}$ is defined in (5). The new proposed green receiver is formulated to minimize the power consumption with respect to the TSE constraints, which is expressed as

$$\min_{\mathbf{r}^{(\tilde{M})},\, \tilde{M}} \quad P_T^{(\tilde{M})} \tag{7}$$

$$s.t.\ \Theta_T^{(\tilde{M})} \geq \Theta_{con}, \tag{8}$$

$$and \ \sum_{i=1}^{b_{max}} r_i = \tilde{M}, \quad r_1, r_2, \cdots, r_{b_{max}} \geq 0, \tag{9}$$

where $\tilde{M}$ is the number of active receive antennas and $\tilde{M} \leq M$; and $\Theta_{con} = \eta \times \Theta_{full}^{(M)}$ and $0 < \eta \leq 1$, in which $\Theta_{full}^{(M)}$ is the TSE for all M receive antennas that are active and connected to full-resolution ADCs. Note that the ADC with full resolution represents that its ADC resolution coefficient is equal to $c_{b_{max}}$ (*i.e.* $a_m = c_{b_{max}} \approx 1$). $c_{b_{max}}$ is defined in Table 3. Further, $\Theta_T^{(\tilde{M})}$ and $P_T^{(\tilde{M})}$ can be computed by (5) and (6), respectively.

The issue in (7)-(9) is a nonlinear integer programming problem, and the complexity using exhaustive search to obtain the optimal solution is $\mathcal{O}(\sum_{m=1}^{M} m^{b_{max}})$. For massive MIMO systems, since M is generally large, the complexity using exhaustive search is immense. Hence, low-complexity methods are needed. In this sub-section, a low complexity method, namely GR-TSE, is proposed. The basic idea of the proposed scheme is described as follows: first, let the number of active receive antennas, $\tilde{M} = M$, and then search the correspondingly optimal candidate of the multi-level-mixed-ADC resolution vector $\mathbf{r}^{(\tilde{M})}$. Second, decrease $\tilde{M}$ by 1 (i.e. let $\tilde{M} = \tilde{M} - 1$) and search the correspondingly optimal candidate $\mathbf{r}^{(\tilde{M})}$. Third, repeat these mechanisms to obtain all optimal multi-level-mixed-ADC candidates for different $\tilde{M}$. Last, the multi-level-mixed-ADC candidate $\mathbf{r}^{(\tilde{M})}$ and corresponding $\tilde{M}$, which achieve the minimum power consumption, are chosen as the optimal solution for (7)-(9). For ease of reading, the flowchart of the proposed new green receiver, namely, GR-TSE, is plotted in Fig. 1. In addition, the function blocks of the flowchart are described as follows:

1) BLOCK 0: INITIALIZATION

First, let $\tilde{M} = M$ and the initial value of the $b_{max} \times 1$ multi-level-mixed-ADC candidate $\mathbf{r}^{(\tilde{M})} = [0, 0, \cdots, 0, M]^T$. Note that $\mathbf{r}^{(\tilde{M})}$'s entry values represent that all M receive antennas are active and each antenna has a full-resolution ADC. With $\mathbf{r}^{(\tilde{M})}$, (5) and (6) are computed to obtain the TSE and power consumption, which are denoted as $\Theta_T^{(\tilde{M})}$ and $P_T^{(\tilde{M})}$, respectively. Note that the TSE in (4) is defined as $\Theta_T^{(\tilde{M})} = \sum_{k=1}^{K} R_k^{(\tilde{M})}$. Thus $\tilde{M} = M$ and $\mathbf{r}^{(\tilde{M})} = [0, 0, \cdots, 0, M]^T$, $\Theta_T^{(\tilde{M})}$ and $P_T^{(\tilde{M})}$ are the TSE and the corresponding power consumption, respectively, for all M active receive antennas and ADCs with full resolution. Hence, let $\Theta_{full}^{(M)} = \Theta_T^{(\tilde{M})}$ and $P_{full}^{(M)} = P_T^{(\tilde{M})}$, where $P_{full}^{(M)}$ represents the power consumption for M active receive antennas with full-resolution ADCs. In addition, let the tentative power consumption $P_{outer} = P_{full}^{(M)}$, which will be employed as the benchmark of the following solution search. Further, denote $\mathbf{r}_{inner,opt}$ and $\mathbf{r}_{outer,opt}$ as the optimal multi-level-mixed-ADC resolution vectors for the Inner Search Loop (described in Block 3) and the Outer Search Loop (described in Block 1), respectively, and then let their initial values be $\mathbf{r}^{(\tilde{M})}$.

Note that $\tilde{M}$ is utilized for the loop variable of the Outer Search Loop and its initial value is M. Furthermore, the value of $\tilde{M}$ represents the number of the active receive antennas and will be applied to search the correspondingly optimal multi-level-mixed-ADC resolution candidate $\mathbf{r}^{(\tilde{M})}$.

2) BLOCK 1: OUTER SEARCH LOOP: PROGRESSIVELY TURN OFF ACTIVE RECEIVE ANTENNAS

The goal of Block 1 is to search the optimal multi-level-mixed-ADC Resolution candidates $\mathbf{r}_{outer,opt}$ for a different number of active receive antennas. First, at each beginning of this loop, the multi-level-mixed-ADC candidate will be initially set to $\mathbf{r}^{(\tilde{M})} = [0, 0, \cdots, 0, \tilde{M}]^T$, $1 \leq \tilde{M} \leq M$, which indicates that the receiver has $\tilde{M}$ active antennas, and each antenna has a full-resolution ADC. Second, with $\mathbf{r}^{(\tilde{M})}$, (6) is re-computed to obtain the corresponding power consumption, which is $P_T^{(\tilde{M})}$. Further, let the flag $\tau_1 = 0$; it will be toggled to 1 when the power consumption is less than P_{outer} at the following Block 3. At each end of the Outer Search Loop, the value of $\tilde{M}$ is decreased by 1 for the next loop iteration.

For the initialization of the Inner Search Loop (described at Block 2), let the loop variable $n = b_{max}$; it will be successively decreased at each iteration of Block 2. Denote P_{inner} as the benchmark of power consumption for the Inner Search Loop and let $P_{inner} = P_T^{(\tilde{M})}$ for the initial value.

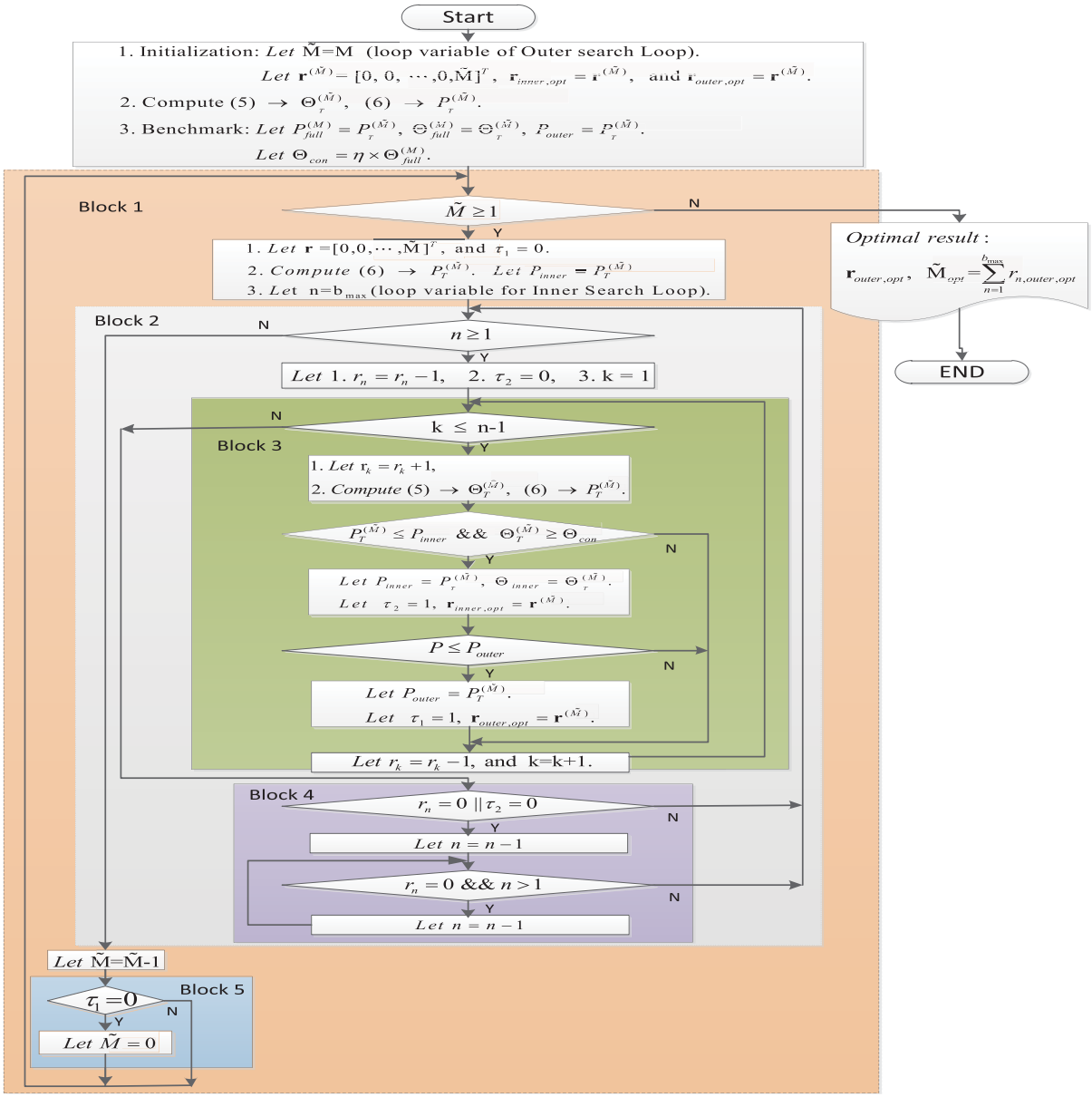

FIGURE 1. Flowchart of the proposed GR-TSE.

3) BLOCK 2: INNER SEARCH LOOP: PROGRESSIVELY CHANGE RESOLUTION BITS *n*

At each iteration of Block 2, GR-TSE, as DSDP [1], obtains the optimal multi-level-mixed-ADC resolution vector $\mathbf{r}_{inner,opt}$ for the corresponding n. First, at each iteration of the Inner Search Loop, decrease the value of the nth entry of r by 1 (*i.e.* $r_n = r_n - 1$). Further, denote $\tau_2 = 0$, which is used to represent that the optimal multi-level-mixed-ADC resolution candidate has not been obtained. Next, iteratively repeat the following **Block 3**, **Block 4**, and **Block 5** until $n = 1$.

4) BLOCK 3: SEARCH THE OPTIMAL MULTI-LEVEL-MIXED-ADC CANDIDATE

The goal of Block 3 is to obtain $\mathbf{r}_{inner,opt}$ by successively changing the entry values of the multi-level-mixed-ADC candidate $\mathbf{r}^{(\tilde{M})}$ under given $\tilde{M}$ active receive antennas. First, let $k = 1, 2, \cdots, n-1$ and iteratively conduct the following three stages: 1) Let $r_k = r_k + 1$. Second, with this new candidate of the multi-level-mixed-ADC resolution $\mathbf{r}^{(\tilde{M})}$, compute (5) to find the corresponding TSE, which is denoted as $\Theta_T^{(\tilde{M})}$. Calculate (6) for the corresponding power consumption and denote the result as $P_T^{(\tilde{M})}$; 2) Check if $P_T^{(\tilde{M})} \leq P_{inner}$ and $\Theta_T^{(\tilde{M})} \geq \Theta_{con}$. If the result of the check is true, the change of r_k at Stage 1 can further achieve less power consumption and fit the TSE constraint. This better candidate for the power consumption and TSE constraint needs to be recorded. Hence, let $\tau_2 = 1$, $P_{inner} = P_T^{(\tilde{M})}$, and $\mathbf{r}_{inner,opt} = \mathbf{r}^{(\tilde{M})}$. Similarly, if $P_T^{(\tilde{M})} \leq P_{outer}$, let $\tau_1 = 1$, $P_{outer} = P_T^{(\tilde{M})}$, and $\mathbf{r}_{outer,opt} = \mathbf{r}^{(\tilde{M})}$; 3). Let $r_k = r_k - 1$, which is used to restore the value of r_k that changed at Stage 1.

5) BLOCK 4: SPEED UP INNER SEARCH LOOP

Block 4 is employed to accelerate the Inner Search Loop. The mechanisms of Block 4 include two stages: 1) When $r_n = 0$ or $\tau_2 = 0$, let $n = n - 1$. 2) Use the subsequent while loop to test ($r_n = 0$) or ($n \geq 1$), and let $n = n - 1$ if the result of the test is true. For example, we assume that the multi-level-mixed-ADC candidate is $\mathbf{r}^{(\tilde{M})} = [0,\ 0,\ 2,\ 0,\ 4,\ 120,\ 0,\ 0]^T$. In addition, we assume that $b_{max} = 8$ and $M = 128$. The active receive antennas $\tilde{M} = \sum_{n=1}^{b_{max}} r_n = 126$. First, at Stage 1, since $r_8 = 0$ satisfies the condition (*i.e.* $r_n = 0$), let $n = n - 1(= b_{max} - 1) = 7$. Second, r_7 is also zero, and hence, it does not need to conduct Block 3 to compute the corresponding power consumption and TSE constraint. As a result, the Inner Search Loop can be accelerated. Furthermore, the while loop (i.e., Stage 2) is applied to obtain the next non-zero r_n. Because $n = 7$, which causes the loop condition $r_n = 0$ to be true, conduct $n = n - 1$; the result is $n = 6$. Next, $r_n = 120$ (*i.e.* $r_6 = 120$). Note that $n = 6$ and $r_n = 120$ represent that 120 receive antennas are active and each of the antennas' ADC resolutions is 6 bits. In addition, the total number of active receive antennas $\tilde{M} = r_3 + r_5 + r_6 = 2 + 4 + 120 = 126$.

6) BLOCK 5: SPEED UP OUTER SEARCH LOOP

In Block 5, if τ_1 is 0, let the loop variable $\tilde{M}$ of The Outer Search Loop be zero. As a result, the residual iterations of The Outer Search Loop will be stopped. The residual searches of Outer Search Loop are stopped because the optimal resolution candidate cannot be obtained with the lesser number of active receive antennas, which will be proven in Appendix. Therefore, Block 5 can accelerate the Outer Search Loop. The optimal result for the multi-level-mixed-ADC resolution vector is $\mathbf{r}_{outer,opt}$. In addition, the correspondingly optimal number of active receive antennas is $\tilde{M}_{opt} = \sum_{n=1}^{b_{max}} r_{n,outer,opt}$, where $r_{n,outer,opt}$ is the nth entry of $\mathbf{r}_{outer,opt}$. The correspondingly optimal TSE and power consumption are denoted as $\Theta_{T,opt}^{(\tilde{M})}$ and $P_{T,opt}^{(\tilde{M})}$, respectively.

The proposed scheme is not an exhaustive search approach for the following two reasons. First, Block 2 of the proposed scheme is similar to the DSDP method [1], which is a dynamic programming approach. The worst-case complexity for testing the multi-level-mixed-ADC resolution candidates is $\mathcal{O}(mb_{max}^2)$, where m is the number of active receive antennas. Second, the proposed scheme uses Block 5 to perform the search only from $m = M$ to $m = \tilde{M}$. Hence, the total complexity for the proposed GR-TSE to obtain the optimal solution is $\mathcal{O}(\sum_{m=\tilde{M}}^{M} mb_{max}^2)$, which is less than the complexity of exhaustive search, $\mathcal{O}(\sum_{m=1}^{M} m^{b_{max}})$.

B. GREEN RECEIVER WITH PER-USER SPECTRAL EFFICIENCY (GR-PUSE) CONSTRAINT

In this subsection, each user with their individual SE demand is considered. The second green receiver is formulated to minimize power consumption with respect to each user's individual spectral efficiency (SE) constraints, which are still aimed at finding the optimal solution of the multi-level-mixed-ADC resolution vector and the corresponding number of active receive antennas. First, similar to (7)-(9) for GR-TSE, the second green receiver with PUSE (namely, GR-PUSE) can be formulated as

$$\min_{\mathbf{r}^{(\tilde{M})},\ \tilde{M}} \quad P_T{}^{(\tilde{M})} \tag{10}$$

$$\begin{aligned} s.t.\ & R_1^{(\tilde{M})} \geq \eta_1 \times \Theta_{cos,1}, \\ & R_2^{(\tilde{M})} \geq \eta_2 \times \Theta_{cos,2}, \\ & \vdots \\ & R_K^{(\tilde{M})} \geq \eta_K \times \Theta_{cos,K}, \end{aligned} \tag{11}$$

$$and \quad \sum_{i=1}^{b_{max}} r_i = \tilde{M},\ \ r_1, r_2, \cdots, r_{b_{max}} \geq 0, \tag{12}$$

where $0 < \eta_k \leq 1, k = 1, \cdots, K$. $\Theta_{con,k} = \eta_k \times \Theta_{full,k}^{(M)}$ is the PUSE constraint for user k, in which $\Theta_{full,k}^{(M)}$ is the SE of user k for the receiver with M active antennas, whose ADCs are full-resolution ADCs. Further, to solve (10)-(12), a new search method is proposed with similar procedures and function blocks as GR-TSE but with slight modifications. The slight modifications include

1) BLOCK 0: INITIALIZATION

The modification for the initialization block of GR-PUSE is described as follows: in the initialization, due to $\tilde{M} = M$ and $\mathbf{r}^{(\tilde{M})} = [0, 0, \cdots, 0, M]^T$, this modification represents that all M receive antennas are active and all ADCs have full resolution. The corresponding SE for user k, $R_k^{(\tilde{M})}, k = 1, \cdots, K$, can be computed by (5). Although the result is denoted as $R_k^{(\tilde{M})}$, it also represents that the corresponding SE for all M receive antennas are active and all ADCs have full resolution. Hence, let $\Theta_{full,k}^{(M)} = R_k^{(M)}, k = 1, \cdots, K$ in the initial step. Apart from this modification, the residual part of the initialization of GR-PUSE is similar to the corresponding initialization of GR-TSE.

2) BLOCK 3: SEARCH THE OPTIMAL MULTI-LEVEL-MIXED-ADC RESOLUTION VECTOR

1) Due to the PUSE constraints shown in (11), compute (5) for each user and denote it as $R_k^{(\tilde{M})}$ for user $k, k = 1, \cdots, K$. 2) Respectively, change GR-TSE's parameters $\Theta_T^{(\tilde{M})}$ and Θ_{con} to $R_k^{(\tilde{M})}$ and $\Theta_{con,k}, k = 1, \cdots, K$ for GR-PUSE.

For GR-TSE, the optimal results of GR-PUSE for the multi-level-mixed-ADC resolution vector and the corresponding number of active receive antennas are $\mathbf{r}_{outer,opt}$ and $\tilde{M}_{opt} = \sum_{i=1}^{b_{max}} r_{i,outer,opt}$, respectively.

IV. SIMULATIONS RESULTS AND COMPLEXITY ANALYSIS

In this section, computer simulations and complexity analysis were conducted to verify the performance of the two proposed green receivers. As [19], a circular cell with a radius of 1 km is considered, in which $K = 10$ users are active and randomly located in a ring region with the distance to the BS, $l_i = 100$ m, $i = 1, \cdots, K$. In addition, it is

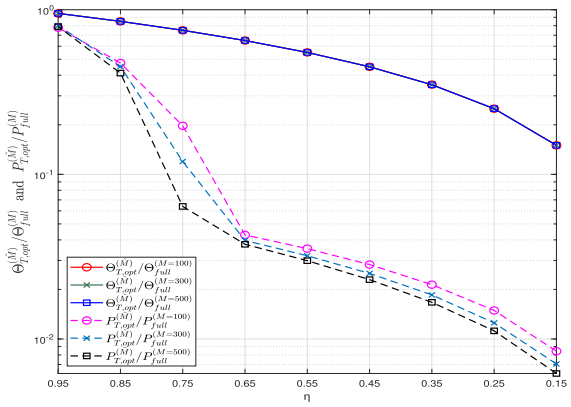

FIGURE 2. Performance results of GR-TSE.

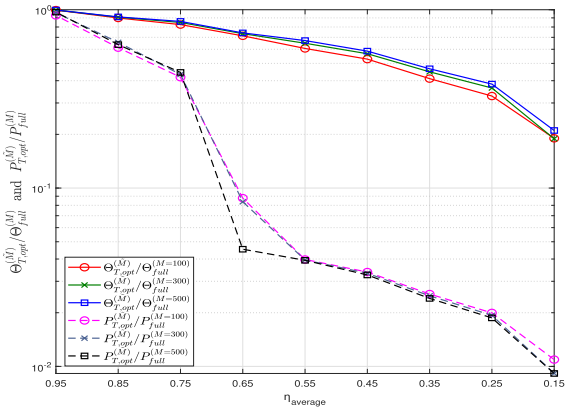

FIGURE 3. Performance results of GR-PUSE.

TABLE 4. The optimal results of GR-TSE with $\eta = 0.85$.

	r_1	r_2	r_3	r_4	r_5	r_6	r_7	r_8
$M = 100, \tilde{M} = 99$	45	1	0	3	1	3	4	42
$M = 300, \tilde{M} = 299$	164	0	3	1	0	3	2	126
$M = 500, \tilde{M} = 500$	302	1	1	1	1	2	1	191

TABLE 5. The optimal results of GR-TSE with $\eta = 0.75$.

	r_1	r_2	r_3	r_4	r_5	r_6	r_7	r_8
$M = 100, \tilde{M} = 100$	78	2	0	1	1	1	3	14
$M = 300, \tilde{M} = 300$	268	2	0	3	0	3	3	21
$M = 500, \tilde{M} = 500$	481	2	2	0	2	2	4	7

TABLE 6. The optimal results of GR-TSE with $\eta = 0.65$.

	r_1	r_2	r_3	r_4	r_5	r_6	r_7	r_8
$M = 100, \tilde{M} = 94$	91	2	1	0	0	0	0	0
$M = 300, \tilde{M} = 263$	262	0	1	0	0	0	0	0
$M = 500, \tilde{M} = 415$	412	1	2	0	0	0	0	0

TABLE 7. The optimal results of GR-PUSE with $\eta_{average} = 0.85$.

	r_1	r_2	r_3	r_4	r_5	r_6	r_7	r_8
$M = 100, \tilde{M} = 100$	35	1	3	0	3	0	3	55
$M = 300, \tilde{M} = 300$	107	2	1	2	1	1	2	184
$M = 500, \tilde{M} = 500$	181	1	0	3	0	2	2	311

TABLE 8. The optimal results of GR-PUSE with $\eta_{average} = 0.75$.

	r_1	r_2	r_3	r_4	r_5	r_6	r_7	r_8
$M = 100, \tilde{M} = 99$	61	0	2	3	1	3	0	29
$M = 300, \tilde{M} = 300$	206	2	2	3	0	2	0	85
$M = 500, \tilde{M} = 500$	366	0	3	0	0	1	4	126

TABLE 9. The optimal results of GR-PUSE with $\eta_{average} = 0.65$.

	r_1	r_2	r_3	r_4	r_5	r_6	r_7	r_8
$M = 100, \tilde{M} = 99$	96	1	2	0	0	0	0	0
$M = 300, \tilde{M} = 295$	294	1	0	0	0	0	0	0
$M = 500, \tilde{M} = 483$	483	0	0	0	0	0	0	0

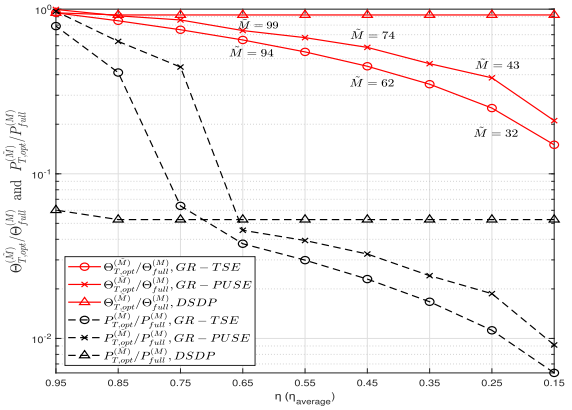

FIGURE 4. Performance comparisons with $M = 100$.

assumed that the shadow-fading deviation $\sigma_{shad} = 4.9$ dB for log-normal random variable z_i, and the path loss exponent γ is 2.1. As [19], the corresponding large-scale fading matrix $\mathbf{L}$ is diag{13.13, 6.49, 11.01, 4.87, 29, 8.69, 50.02, 96, 1.24, 41.04} $\times 10^{-4}$ for the simulations. In addition, as shown in [1], set $P_d = 10^{-7}$ Watt, $P_b = 10^{-4}$ Watt, and $P_c = 10^{-3}$ Watt in (3). The performance results of GR-TSE, *i.e.* the ratios for $\Theta^{(\tilde{M})}_{T,opt}/\Theta^{(M)}_{full}$ ($P^{(\tilde{M})}_{T,opt}/P^{(M)}_{full}$) versus η, are shown in Fig. 2. Note that $\Theta^{(\tilde{M})}_{T,opt}$ and $P^{(\tilde{M})}_{T,opt}$ are the optimal $\Theta^{(\tilde{M})}_{T}$ and $P^{(\tilde{M})}_{T}$, respectively. In addition, to provide more insight into GR-TSE, the optimal results for $\eta = 0.85, 0.75$, and 0.65 are shown in Tables 4, 5 and 6, respectively. For GR-PUSE, the ratios for $\Theta^{(\tilde{M})}_{T,opt}/\Theta^{(M)}_{full}$ ($P^{(\tilde{M})}_{T,opt}/P^{(M)}_{full}$) versus $\eta_{average}$ are shown in Fig. 3, and the corresponding results are shown in Tables 7–9. Note that $\eta_{average}$ is the average of $\eta_1, \cdots \eta_K$. For ease of simulation, η_k in (11), $k = 1, \cdots, K$, is assumed to be a continuous random variable that is uniformly distributed in the interval $[0.95\eta_{average}, 0.15\eta_{average}]$. Furthermore, Figs. 4-7 show the performance comparisons of GR-TSE, GR-PUSE, and DSDP [1]. A complexity analysis for the previously mentioned methods is conducted to further assess the performance. For ease of comparison, the complexity analysis with numerical results is summarized in Table 10.

A. GR-TSE

Three different numbers of receive antennas for GR-TSE are considered, including $M = 100$, $M = 300$, and $M = 500$. The performance results of the ratios for $\Theta^{(\tilde{M})}_{T,opt}/\Theta^{(M)}_{full}$

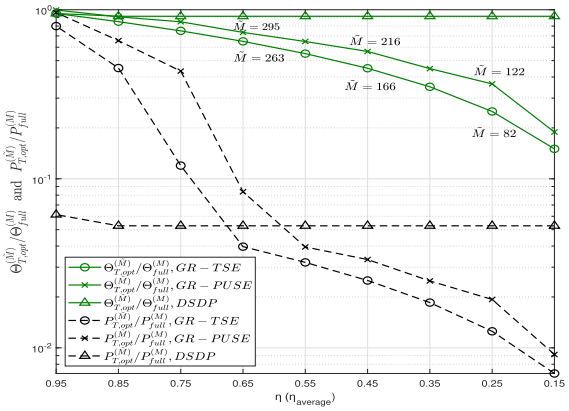

FIGURE 5. Performance comparisons with $M = 300$.

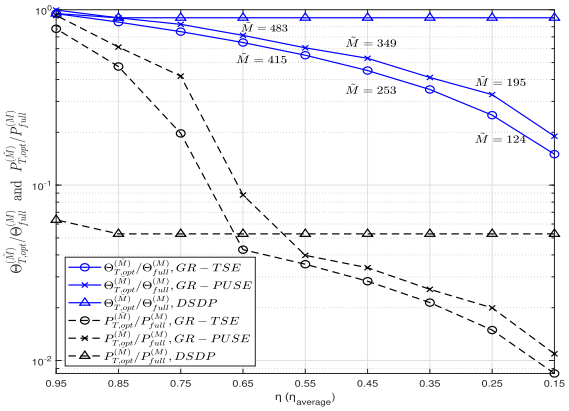

FIGURE 6. Performance comparisons with $M = 500$.

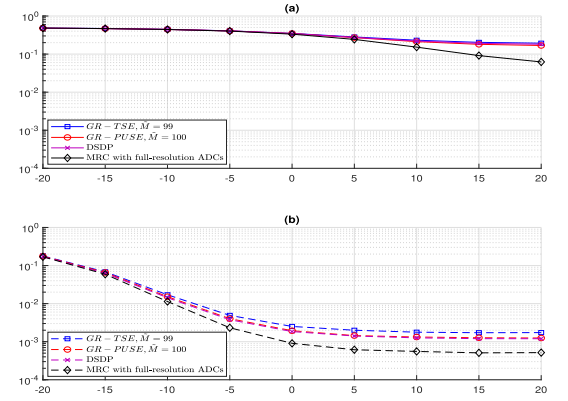

FIGURE 7. Comparison of the BER versus the SNR for $M = 100$, $\eta(\eta_{average}) = 0.85$ (a) with the large-scale fading effect (b) without the large-scale fading effect.

$(P_{T,opt}^{(\tilde{M})}/P_{full}^{(M)})$ are shown in Fig. 2. From Fig. 2, we can observe that both $\Theta_{T,opt}^{(\tilde{M})}/\Theta_{full}^{(M)}$ and $P_{T,opt}^{(\tilde{M})}/P_{full}^{(M)}$ decrease as η decreases. This finding can be explained by (8); smaller η will result in less Θ_{con}, and hence, less $\Theta_{T}^{(\tilde{M})}$. Furthermore, with (5), lower TSE $\Theta_{T}^{(\tilde{M})}$ is produced from a reduction in the number of ADC resolutions, which leads to less power consumption $P_{T}^{(\tilde{M})}$ in (6). In addition, we can further observe that the results of $\Theta_{T,opt}^{(\tilde{M})}/\Theta_{full}^{(M)}$ for a different number of receive

TABLE 10. The number of tested resolution vectors, $M = 300$.

	$\eta = 0.85$	$\eta = 0.75$	$\eta = 0.65$
Exhaustive search	6.561×10^{19}	6.561×10^{19}	6.561×10^{19}
DSDP [1]	6300	6300	6300
proposed GR-TSE	6300,$\tilde{M} = M$	6300,$\tilde{M} = M$	224637,$\tilde{M} = 263$
proposed GR-PUSE	6300,$\tilde{M} = M$	6300,$\tilde{M} = M$	37485,$\tilde{M} = 295$

antennas are almost equivalent. However, for power consumption, the corresponding results of $P_{T,opt}^{(\tilde{M})}/P_{full}^{(M)}$ decreases as the number of receive antennas increases, which represents that GR-TSE can achieve higher power efficiency with additional receive antennas.

To provide more insight into GR-TSE, the optimal results of the multi-level-mixed-ADC resolution vectors for receive antennas $M = 100$, $M = 300$, and $M = 500$ are shown in Tables 4, 5 and 6 respectively. First, in Table 4, as $\eta = 0.85$, we can observe that regardless of the values of M, almost all receive antennas are active, *i.e.* $\tilde{M} \approx M$. In addition, the results also show that r_1 and r_8 are the two main quantities of the multi-level-mixed-ADC resolution vectors, which implies that these ADC deployments of GR-TSE are similar to two-level-mixed-ADC [19].

Second, change $\eta = 0.85$ to 0.75; the corresponding optimal results are shown in Table 5. From Table 5, we can also receive a conclusion similar to $\eta = 0.85$, including the conclusion that GR-TSE's ADC resolution vectors are similar to two-level mixed ADC. However, the values of r_1 are much larger than those of r_8's regardless of the number of receive antennas. The result is attributed to the notion that changing $\eta = 0.85$ to 0.75, the requirement of TSE becomes less. GR-TSE can use more quantities of low-resolution ADCs instead of high-resolution ADCs. As a result, power consumption is reduced. Furthermore, change $\eta = 0.75$ to 0.65, and show the corresponding optimal results in Table 6. From Table 6, we can observe that the values of r_1 are almost equal to the number of active receive antennas $\tilde{M}$. This finding means that almost all active receive antennas are connected with 1-bit-resolution ADCs, which implies that GR-TSE now configures the receiver with one-level low-resolution ADCs [18]. Moreover, as shown in Table 6, the receive antennas $M = 100$, $M = 300$, and $M = 500$ are only active with $\tilde{M} = 94$, $\tilde{M} = 263$, and $\tilde{M} = 415$, respectively. This finding represents that GR-TSE can turn off the redundant antennas to reduce power consumption as the requirement of TSE decreases.

From Table 4 and Table 5, we observe that $\tilde{M} \approx M$ in some scenarios, which implies that all receive antennas are active. Further, for example, consider the results on the first row of Table 4 for the ADC deployment of the proposed GR-TSE. The corresponding power consumption can be computed by (6) and expressed as $P_{T,opt}^{(\tilde{M})} = 10^{-7} \times 2 \times 99 \times 10 + 10^{-4} \times (45 \times 2^1 + 2^2 + 3 \times 2^4 + 2^5 + 3 \times 2^6 + 4 \times 2^7 + 42 \times 2^8) + 10^{-3} \times 99 = 1.2652$ Watt. However, the power consumption for the receiver with full-resolution ADCs is $P_{full}^{(M)} = 10^{-7} \times 2 \times 100 \times 10 + 10^{-4} \times 100 \times 2^8 + 10^{-3} \times 100 = 2.6602$ Watt. These practical Results reveal that the proposed GR-TSE can

reduce power consumption, compared to the receiver with full-resolution ADCs. In addition, we can also draw similar conclusions from other scenarios of Tables 4-5. Furthermore, we can observe from some results of Table 4 and Table 5 that the numbers of active receive antennas $\tilde{M}$ of the GR-TSE are almost equal to the number of all receive antennas, M, which represents that GR-TSE does not conduct Block 5. As a result, compared to the DSDP, the proposed GR-TSE does not require extra computations in these scenarios.

B. GR-PUSE

The same settings of Fig. 2 are also considered for GR-PUSE and the performance results are shown in Fig. 3. From Fig. 3, we can receive similar conclusions as those from Fig. 2. The conclusions include: as $\eta_{average}$ becomes small, $\Theta_{T,opt}^{(\tilde{M})}/\Theta_{full}^{(M)}$ and $P_{T,opt}^{(\tilde{M})}/P_{full}^{(M)}$ both decrease; and the results of $P_{T,opt}^{(\tilde{M})}/P_{full}^{(M)}$ slightly reduce as the number of receive antennas increases. However, as the number of receive antennas M increases, the results of $\Theta_{T,opt}^{(\tilde{M})}/\Theta_{full}^{(M)}$ also slightly reduce at the same $\eta_{average}$, which are different from those of the GR-TSE.

Furthermore, conduct GR-PUSE with the same settings in Tables 4-6. The corresponding results are shown in Tables 7-9. From Table 7, we also draw conclusions similar to those in Table 4: as $\eta_{average} = 0.85$, all receive antennas for GR-PUSE are active. From the optimal results of the multi-level-mixed-ADC resolution vector, the active receive antennas are mainly connected with one-bit-resolution ADCs and full-resolution ADCs. In particular, as $\eta_{average}$ changes to 0.75, we can observe from the results of Table 8 that one-bit resolution and full resolution are still the two main entries of the multi-level-mixed-ADC resolution vector of GR-PUSE. In addition, the quantities of one-bit-resolution is higher than those of full resolution. Further, Table 9 shows that the GR-PUSE receiver almost uses one-bit-resolution ADCs only. In addition, similar to GR-TSE, as $\eta_{average}$ is changed to 0.65, the optimal number of active receive antennas for GR-PUSE are reduced to $\tilde{M} = 99$, $\tilde{M} = 295$, and $\tilde{M} = 483$ for $M = 100$, 300 and 500, respectively, which also represents that the GR-PUSE turns off some redundant antennas for power saving.

C. COMPARISONS

To compare the performance of GR-TSE, GR-PUSE, and DSDP [1], the receive antennas $M = 100$, $M = 300$, and $M = 500$, respectively, are considered, and the results of power consumption and TSE for the previously mentioned three schemes are shown in Figs. 4-6. From the figures, we can observe that the $\Theta_{T,opt}^{(\tilde{M})}/\Theta_{full}^{(M)}$ and $P_{T,opt}^{(\tilde{M})}/P_{full}^{(M)}$ of DSDP almost remain unchanged. For DSDP, $\tilde{M} = M$ because no mechanism in DSDP turns off the receive antennas. However, for different η ($\eta_{average}$), the proposed GR-TSE (GR-PUSE) can have different ratios $\Theta_{T,opt}^{(\tilde{M})}/\Theta_{full}^{(M)}$ and $P_{T,opt}^{(\tilde{M})}/P_{full}^{(M)}$. Furthermore, for the same ratio value of $\Theta_{T,opt}^{(\tilde{M})}/\Theta_{full}^{(M)}$, GR-PUSE consumes slightly less power than GR-TSE. For example, $\Theta_{T,opt}^{(\tilde{M})}/\Theta_{full}^{(M)} = 0.9$ at Fig. 4, the $P_{T,opt}^{(\tilde{M})}/P_{full}^{(M)}$ for GR-TSE and GR-PUSE are 0.009 and 0.0087, respectively, which represents that the power efficiency of GR-PUSE is slightly higher than that of GR-TSE.

To gain more insight into the proposed green receivers, we further compare the bit error rate (BER) performance of the three previously mentioned schemes. The scenario ($M = 100$, $\eta(\eta_{average}) = 0.85$) is considered. In addition, we also simultaneously assume that $K = 10$ users send quadrature phase-shift keying (QPSK) symbols [20] to the receiver. Due to MRC detection, which is employed for the previously mentioned three methods, the MRC receiver with $M = 100$ receive antennas and all ADCs with full resolution is also conducted as the performance benchmark. The results are shown in Figs. 7(a)-(b). From Fig. 7(a), we observe that the BER performance of the proposed schemes and DSDP degrades, because the three methods experience quantization noise because their receivers use ADCs with lower resolution. However, the BER performances of the three schemes are similar. Note that the mechanism of power control will be conducted at the BS receivers to compensate the large-scale fading effect. Hence, we further assume that the mechanism of perfect power control is conducted at the system, which generates the large-fading matrix $\mathbf{L} = \mathbf{I}$. The corresponding BER performance results are shown in Fig. 7(b). From Fig. 7(b), we can observe that the proposed two schemes and DSDP perform close and near to BER $= 0.001$ as SNR ≥ 5 dB. Therefore, with the help of power control, the BER performance results of the proposed schemes can be further improved.

Next, the computational complexity of the proposed schemes is assessed. First, note that the number of tested resolution vectors is the main role, which dominates the amount of computational complexity of the methods. Further, in [1], the upper bound of the number of tested vectors for DSDP has been shown as $\frac{(b_{max}-1)(b_{max}-2)M}{2}$. For the proposed two schemes, their amounts are both $\sum_{m=\tilde{M}}^{M} \frac{(b_{max}-1)(b_{max}-2)m}{2}$. To gain more insight into these expressions, we substituted some practical values of Tables 4-9 into them. The results are shown in Table 10. In addition, the number of tested vectors for exhaustive search, *i.e.* $M^{b_{max}}$, is also provided in Table 10 for comparison. The results in Table 10 show that as $\eta = 0.85$ and 0.75, the proposed green schemes and DSDP test the same number of resolution vectors, and hence, their computational complexities are almost equal. As η is changed to 0.65, the two proposed schemes need to test more resolution vectors than DSDP. However, in this scenario, the proposed schemes almost use low-resolution ADCs and turn off redundant receive antennas. As a result, the proposed schemes can save more power than DSDP.

V. CONCLUDING REMARKS

In this paper, we have proposed two green receivers with the optimal multi-level-mixed-ADC resolution vectors and

corresponding number of active receive antennas for massive MIMO systems. The proposed schemes turn off parts of the receive antennas and separately change the entries of the multi-level-mixed-ADC resolution vector, which is aimed at minimizing the power consumption for given SE constraints. One of the two proposed receivers is subject to the TSE constraint, and the other proposed receiver has the PUSE constraint. With the given SE constraints, the proposed green receiver with the PUSE constraint can consume slightly less power than the green receiver with the TSE constraint. Furthermore, compared to the DSDP method [1], the two proposed green receivers can provide the advantage of the adjustable flexibility of power consumption with different SE requirements. To facilitate the procedure for searching the number of turn-off antennas, the proposed green receivers require more computational complexity than DSDP. Nevertheless, a novel mechanism (Block 5 of the proposed receivers) for accelerating the searching has been designed in the proposed receivers.

Recently, some interesting topics, including channels with spatially correlated [30], [31] and/or detection using zero-forcing (ZF) and successive interference cancellation (SIC) [32], [33] for massive MIMO systems are emerging. However, these topics are beyond the scope of this paper and will be considered in our future works.

APPENDIX

This appendix demonstrates that when the optimal number of active receive antennas $\tilde{M}$ and the corresponding resolution vector $\mathbf{r}^{(\tilde{M})}$ are obtained, $\Theta_T^{(\tilde{M}-1)}$ is always less than the corresponding TSE constraint Θ_{con}. This finding implies that the proposed schemes can stop searching as the optimal $\tilde{M}$ is obtained. For ease of demonstration and without loss of generality, the situation ($K = 1$ and the amount of all receive antennas $M = 2$) is considered. In addition, we also assume the optimal result of $\tilde{M}$ is 2. Due to the definition $\Theta_{con} = \eta \times \Theta_{full}^{(M)}$ and using (4), the corresponding Θ_{con} for $K = 1$ and $M = 2$ can be expressed as

$$\begin{aligned}\Theta_{con} &= \eta \times \Theta_{full}^{(M)} \\ &= \eta \times \log_2\left(1 + \frac{\beta_1((a_1+a_2)^2 + (a_1^2+a_2^2))}{\gamma((a_1+a_2)) - 2\beta_1(a_1^2+a_2^2)}\right) \\ &= \eta \times \log_2\left(1 + \frac{1+6\beta_1}{2\gamma - 4\beta_1}\right) \end{aligned} \tag{13}$$

Note that in (4), $\alpha_1 = (a_1 + a_2)$, $\alpha_2 = (a_1^2 + a_2^2)$, and $\gamma = 1 + 2\beta_1$ for $M = 2$ and $K = 1$. In addition, for $\Theta_{full}^{(M)}$, it represents that the two receive antennas are with full-resolution ADCs, and hence a_1 and a_2 are both equal to 1. Then, (13) can be further simplified as

$$\Theta_{con} = \log_2(1.5 + 3\beta_1)^{\eta} \tag{14}$$

Similarly, the maximum value for $\Theta_T^{(\tilde{M}-1)}$ can be readily computed with $K = 1$ and $\eta = 1$. Note that due to the previous assumption of the optimal $\tilde{M} = 2$, the maximum value for $\Theta_T^{(\tilde{M}-1)}$ is achieved by one active antenna with a full-resolution ADC. Therefore, using (4), the maximum value for $\Theta_T^{(\tilde{M}-1)}$ can be expressed as

$$\Theta_{T,max}^{(1)} = \log_2(1 + 2\beta_1) \tag{15}$$

From Section IV, it is known that $\beta_i \ll 1, i = 1 \cdots K$. In addition, for the comparison of (14) and (15), we consider that the log function is monotonically increasing and $(1.5 + 3\beta_1)^{\eta} > (1 + 2\beta_1)$ if $0 < \eta \leq 1$. We can further obtain $\Theta_{T,max}^{(1)} < \Theta_{con}$, which implies that the proposed schemes do not need to conduct searching as the number of active antennas is less than the optimal $\tilde{M} = 2$. Furthermore, with some complicated manipulations, the same conclusions can also be obtained for $M \geq 3$ and $K \geq 2$.

REFERENCES

[1] Q. Ding and Y. Jing, "Receiver energy efficiency and resolution profile design for massive MIMO uplink with mixed ADC," *IEEE Trans. Veh. Technol.*, vol. 67, no. 2, pp. 1840–1844, Feb. 2018.

[2] D. Wang, D. Chen, B. Song, N. Guizani, X. Yu, and X. Du, "From IoT to 5G I-IoT: The next generation IoT-based intelligent algorithms and 5G technologies," *IEEE Commun. Mag.*, vol. 56, no. 10, pp. 114–120, Oct. 2018.

[3] A. Yadav and O. A. Dobre, "All technologies work together for good: A glance at future mobile networks," *IEEE Wireless Commun.*, vol. 25, no. 4, pp. 10–16, Aug. 2018.

[4] V. W. S. Wong, R. Schober, D. W. K. Ng, and L.-C. Wang, *Key Technologies for 5G Wireless Systems*. Cambridge, U.K.: Cambridge Univ. Press, 2017.

[5] T. Wei, W. Feng, J. Wang, N. Ge, and J. Lu, "Exploiting the shipping lane information for energy-efficient maritime communications," *IEEE Trans. Veh. Technol.*, vol. 68, no. 7, pp. 7204–7208, Jul. 2019.

[6] A. Morgado, K. M. S. Huq, S. Mumtaz, and J. Rodriguez, "A survey of 5G technologies: Regulatory, standardization and industrial perspectives," *Digit. Commun. Netw.*, vol. 4, no. 2, pp. 87–97, Apr. 2018.

[7] S. Yang and L. Hanzo, "Fifty years of MIMO detection: The road to large-scale MIMOs," *IEEE Commun. Surveys Tuts.*, vol. 17, no. 4, pp. 1941–1988, Nov. 2015.

[8] T. E. Bogale and L. B. Le, "Massive MIMO and mmWave for 5G wireless HetNet: Potential benefits and challenges," *IEEE Veh. Technol. Mag.*, vol. 11, no. 1, pp. 64–75, Mar. 2016.

[9] T. Marzetta, E. Larsson, H. Yang, and H. Quoc, *Fundamentals of Massive MIMO*. Cambridge, U.K.: Cambridge Univ. Press, 2016.

[10] D. Ciuonzo, P. S. Rossi, and S. Dey, "Massive MIMO channel-aware decision fusion," *IEEE Trans. Signal Process.*, vol. 63, no. 1, pp. 604–618, Feb. 2015.

[11] A. Chockalingam and B. S. Rajan, *Large MIMO*. Cambridge, U.K.: Cambridge Univ. Press, 2014.

[12] H. Quoc Ngo, E. G. Larsson, and T. L. Marzetta, "Energy and spectral efficiency of very large multiuser MIMO systems," *IEEE Trans. Commun.*, vol. 61, no. 4, pp. 1436–1449, Apr. 2013.

[13] H. Pirzadeh and A. L. Swindlehurst, "Spectral efficiency of mixed-ADC massive MIMO," *IEEE Trans. Signal Process.*, vol. 66, no. 13, pp. 3599–3613, Jul. 2018.

[14] D. Ha, K. Lee, and J. Kang, "Energy efficiency analysis with circuit power consumption in massive MIMO systems," in *Proc. IEEE PIMRC*, Sep. 2013, pp. 938–942.

[15] K. N. R. S. V. Prasad, E. Hossain, and V. K. Bhargava, "Energy efficiency in massive MIMO-based 5G networks: Opportunities and challenges," *IEEE Wireless Commun.*, vol. 24, no. 3, pp. 86–94, Jun. 2017.

[16] G. Xue, L. Li, G. Lu, H. Tian, and L. Du, "Energy efficiency optimizations of massive MIMO systems with linear receivers," in *Proc. IEEE VTC*, Jun. 2017, pp. 1–5.

[17] P. V. Amadori and C. Masouros, "Interference driven antenna selection for massive multi-user MIMO," *IEEE Trans. Veh. Technol.*, vol. 65, no. 8, pp. 5944–5958, Aug. 2016.

[18] Y. Dong and L. Qiu, "Spectral efficiency of massive MIMO systems with low-resolution ADCs and MMSE receiver," *IEEE Commun. Lett.*, vol. 21, no. 8, pp. 1771–1774, Aug. 2017.

[19] W. Tan, S. Jin, C.-K. Wen, and Y. Jing, "Spectral efficiency of mixed-ADC receivers for massive MIMO systems," *IEEE Access*, vol. 4, pp. 7841–7846, 2016.
[20] J. G. Proakis and M. Salehi, *Digital Communications*, 5th ed. New York, NY, USA: McGraw-Hill, 2008.
[21] G. Scutari, D. P. Palomar, and S. Barbarossa, "The MIMO iterative waterfilling algorithm," *IEEE Trans. Signal Process.*, vol. 57, no. 5, pp. 1917–1935, May 2009.
[22] T.-H. Liu, J.-Y. Jiang, and Y.-S. Chu, "A low-cost MMSE-SIC detector for the MIMO system: Algorithm and hardware implementation," *IEEE Trans. Circuits Syst. II, Exp. Briefs*, vol. 58, no. 1, pp. 56–61, Jan. 2011.
[23] B. J. Chang, Y. H. Liang, K. P. Jhuang, and T. S. Tsai, "Cross-layer channel selection and reward-based power allocation for maximizing system capacity and reward in 4G MIMO wireless communications," in *Proc. ISEEE*, Apr. 2014, pp. 1793–1797.
[24] K. Pham and K. Lee, "Low-complexity SIC detection algorithms for multiple-input multiple-output systems," *IEEE Trans. Signal Process.*, vol. 63, no. 17, pp. 4625–4633, Sep. 2015.
[25] N. P. Le, F. Safaei, and L. C. Tran, "Antenna selection strategies for MIMO-OFDM wireless systems: An energy efficiency perspective," *IEEE Trans. Veh. Technol.*, vol. 65, no. 4, pp. 2048–2062, Apr. 2016.
[26] G. H. Golub and C. F. Van Loan, *Matrix Computations*. 3rd ed. Baltimore, MD, USA: Johns-Hopkins, 1996.
[27] M. Alibakhshikenari, F. Babaeian, B. S. Virdee, S. Aïssa, and L. Azpilicueta, "A comprehensive survey on 'various decoupling mechanisms with focus on metamaterial and metasurface principles applicable to SAR and MIMO antenna systems,'" *IEEE Access*, vol. 8, pp. 192965–193004, 2020.
[28] A. Iqbal, O. A. Saraereh, A. W. Ahmad, and S. Bashir, "Mutual coupling suppression between two closely placed microstrip patches using EM-bandgap metamaterial fractal loading," *IEEE Access*, vol. 6, pp. 2755–2759, 2017.
[29] M. Alibakhshikenari, M. Khalily, B. S. Virdee, C. H. See, R. A. Abd-Alhameed, and E. Limiti, "Mutual-coupling isolation using embedded metamaterial EM bandgap decoupling slab for densely packed array antennas," *IEEE Access*, vol. 7, pp. 51827–51840, 2019.
[30] P. Dong, H. Zhang, Q. Wu, and G. Y. Li, "Spatially correlated massive MIMO relay systems with low-resolution ADCs," *IEEE Trans. Veh. Technol.*, vol. 69, no. 6, pp. 6541–6553, Jun. 2020.
[31] Q. Ding and Y. Lian, "Performance analysis of mixed-ADC massive MIMO systems over spatially correlated channels," *IEEE Access*, vol. 7, pp. 6842–6852, 2019.
[32] Q. Ding and Y. Jing, "SE analysis for mixed-ADC massive MIMO uplink with ZF receiver and imperfect CSI," *IEEE Wireless Commun. Lett.*, vol. 9, no. 4, pp. 438–442, Apr. 2020.
[33] T. Liu, J. Tong, Q. Guo, J. Xi, Y. Yu, and Z. Xiao, "Energy efficiency of massive MIMO systems with low-resolution ADCs and successive interference cancellation," *IEEE Trans. Wireless Commun.*, vol. 18, no. 8, pp. 3987–4002, Aug. 2019.

HOANG-YANG LU received the B.S., M.S., and Ph.D. degrees from the National Taiwan University of Science and Technology, Taipei, in 1991, 1993, and 2007, respectively, all in electronics engineering. From 1993 to 2007, he was a Lecturer with the Department of Electronics Engineering, Lee-Ming Institute of Technology, Taipei. He joined the Digital Technology Department, Kainan University, Taoyuan, Taiwan, in 2007, and the Department of Electronics Engineering, Huafan University, Taipei, in 2008, where he was an Associate Professor. Since 2009, he has been an Assistant Professor with the Department of Electrical Engineering, National Taiwan Ocean University (NTOU). He is currently an Associate Professor with NTOU. His research interests include signal processing, communication systems, and machine learning.

WEI-LIN JIANG was born in Taoyuan, Taiwan, in 1999. He is currently pursuing the bachelor's degree in electrical engineering with National Taiwan Ocean University, Keelung, Taiwan, in 2020. His research interests include wireless communications and massive MIMO systems.

CHENG ZHANG was born in Yilan, Taiwan, in 1999. He is currently pursuing the bachelor's degree in electrical engineering with National Taiwan Ocean University, Keelung, Taiwan, in 2020. His research interests include wireless communications and massive MIMO systems.